Artifact Removed Quantitative Analysis Of Choriocapillaris Flow Voids

M. Giray Ersoz
Biruni University Faculty of Medicine: Biruni Universitesi Tip Fakultesi
Mumin Hocaoglu
Istanbul Retina Institute
Isil Sayman Muslubas
Istanbul Retina Institute
Serra Arf
Istanbul Retina Institute
Erdost Yildiz
Koc University: Koc Universitesi
Murat Karacorlu (mkaracorlu@gmail.com)
Istanbul Retina Institute

Research Article

Keywords: choriocapillaris flow voids, drusen, optical coherence tomography angiography, subretinal fluid.

Posted Date: March 18th, 2021

DOI: https://doi.org/10.21203/rs.3.rs-178394/v1

Abstract

Purpose: To investigate choriocapillaris flow voids (FV) with a new optical coherence tomography angiography (OCTA) image processing strategy to exclude artifacts due to vitreous opacities, subretinal pigment epithelium (sub-RPE) fluid and deposits, and subretinal fluid (SRF) by thresholding the en-face OCT image of the outer retina.

Methods: This retrospective study included 15 eyes with drusen and 15 eyes with SRF. Number (FVn), average area (FVav), and maximum area (FVmax) of FV and the percentage of the nonperfused choriocapillaris area (PNPCA) obtained using the proposed strategy were compared with those obtained by removing only artifacts due to superficial capillary plexus (SCP).

Results: There were three eyes with autosomal dominant drusen and 12 eyes with drusen secondary to non-exudative AMD in the drusen group. SRF group included 15 eyes with active central serous chorioretinopathy. PNPCA, FVav, FVmax, and FVn obtained using the algorithm were significantly lower than those obtained by removing only SCP in both groups (all $p < 0.05$). The algorithm was able to remove 94.7% of artifacts secondary to vitreous opacities and all artifacts secondary to serous pigment epithelial detachments.

Conclusion: Nonperfusion areas of choriocapillaris may be overestimated in eyes with RPE abnormalities and SRF. These areas can be removed using thresholded images of the outer retina en-face OCT scans.

Introduction

Choroid is one of the most highly vascularized tissues of the body. Its main function is to supply oxygen and nutrients to avascular layers of retina and retinal pigment pigment epithelium (RPE). The choroid has three vascular layers: starting from the scleral side, Haller's layer consisting of large-sized vessels, Sattler's layer consisting of medium-sized vessels, and choriocapillaris. The choriocapillaris is a highly anastomosed, lobular, single-layer network of capillaries. It has a thickness of 10 μm at the fovea and 7 μm at the periphery.[1]

Choroid and choriocapillaris abnormalities play an important role in pathogenesis of several retinal diseases such as age-related macular degeneration (AMD), central serous chorioretinopathy (CSC), and polypoidal choroidal vasculopathy (PCV).[2–12] Histological studies revealed that the thickness of choriocapillaris decreases in eyes with AMD and drusenoid deposits are associated with regions of capillary dropout.[8, 10] McLeod et al.[7] reported close association between choriocapillaris degeneration and RPE atrophy in non-exudative AMD with geographic atrophy. They also have found that ischemia due to choriocapillaris degeneration stimulates development of choroidal neovascularization. Studies using indocyanine green angiography revealed the presence of choroidal hyperpermeability and filling defects in eyes with central serous chorioretinopathy (CSC) and polypoidal choroidal vasculopathy (PCV).[2, 9, 11] Drusen-like deposits and RPE abnormalities are colocalized with choriocapillaris filling delay and choroid hyperpermeability in eyes with CSC and their fellow eyes.[4, 6] Enhanced depth imaging (EDI)

spectral domain optical coherence tomography (SD-OCT) and swept-source OCT revealed that the whole choroid is thickened while the inner choroid is attenuated in eyes with CSC and PCV.[2, 3, 5, 12]

Although abnormalities of the choriocapillaris participate pathogenic mechanisms of common retinal diseases, in vivo visualization of the choriocapillaris was not possible until the introduction of OCT-angiography (OCTA). Blood flow appears as bright areas, and flow (signal) void (FV) appears as dark regions in OCTA scans of the choriocapillaris.[13] However, artifacts such as masking, unmasking, motion, projection, and backscattering may cause incorrect signals.[14, 15] Regions of masking artifact due to drusen, pigment epithelium detachment (PED), and some RPE lesions can be excluded,[13] or signal loss secondary to these artifacts can be compensated for with different strategies.[16] However, there has been no appropriate method to overcome all masking and unmasking artifacts due to subretinal fluid (SRF), sub-RPE fluid and deposits, and vitreous opacities.

We performed a new strategy to exclude artifacts due to fluid or deposit accumulation under RPE, and SRF by using thresholding of outer retina en-face OCT scans. In this study, we aimed to compare choriocapillaris FV measurements obtained using our strategy and obtained by removing only artifacts due to the superficial capillary plexus (SCP) in eyes with drusen and eyes with SRF.

Methods

We retrospectively reviewed medical records of patients with drusen and CSC who had been referred to Istanbul Retina Institute from January 2018 to April 2020. 15 eyes with drusen and 15 eyes with SRF were included in the study. Only one eye for each subject was included. Both groups had eyes with PED and vitreous opacities. SRF group had also eyes with drusen-like sub-RPE deposits (Fig. 1).

Medical history, refractive error measurements, and OCTA (RTVue-XR Avanti, Optovue, Fremont, California, USA) images were obtained from the patients' medical records. The study protocol was approved by the Institutional Review Board of Sisli Memorial Hospital, Istanbul. The study adhered to the tenets of the Declaration of Helsinki.

OCTA imaging

En-face OCTA images of the superficial plexus (internal limiting membrane to the inner plexiform layer − 10 μm), outer retina (outer border of outer plexiform layer + 10 μm to Bruch's membrane − 10 μm), and choriocapillaris (Bruch's membrane − 10 μm to Bruch's membrane + 30 μm), and en-face structural OCT images of the outer retina (outer border of outer plexiform layer + 10 μm to Bruch's membrane − 10 μm) were obtained by using RTVue-XR Avanti with a split-spectrum amplitude-decorrelation angiography algorithm (AngioVue software, version 2017.1.0.151; Optovue Inc). All images were 6 × 6 mm and centered on the fovea. The OCTA image of the outer retina was evaluated by using the "remove projection" option.

Image processing

Step 1) En-face OCTA images of the superficial plexus, outer retina, and choriocapillaris, and en-face structural OCT images of the outer retina were extracted as .jpg files. Images were then imported into MATLAB (version 9.8.0 (R2020a), Natick, Massachusetts: The MathWorks Inc.). The MATLAB based stand-alone program and code for analysis are available in https://github.com/erdosty/OCRA/releases/tag/1.46. The edges of images were cut to remove markings of AngioVue software and 5 × 5 mm images centered on the fovea were used for image analysis. A 5000 × 5000 μm (5 × 5 mm) image appears as 500 × 500 pixels (1 pixel = 10 μm).

Step 2) En-face structural OCT images of outer retina have been used to extract artifacts due to hyperreflective and hyporeflective lesions. On en-face structural OCT images of outer retina, MATLAB based algorithm determined the hyperreflective artifacts by gaussian distribution thresholding and the hyporeflective artifacts by maximum entropy thresholding (available in https://github.com/erdosty/OCRA/releases/tag/1.46).[17] Maximum entropy thresholding was applied to the OCTA images of superficial plexus (Fig. 1, 2). Two thresholded images of en-face structural OCT of outer retina and the OCTA image of superficial plexus were merged to obtain images that include all artifacts (Fig. 1–4). Particles function analysis was used to determine the area after exclusion of artifacts.

Step 3) To determine the global threshold of nonperfusion, the mean of the all pixel values in the en-face OCTA image of the outer retina was calculated. Thresholding was applied to the choriocapillaris image by using the global threshold of nonperfusion as previously described (Fig. 1).[13] The choriocapillaris pixels under this threshold point were considered nonperfusion.

Step 4) The image that include all artifacts and the nonperfusion choriocapillaris image were merged and binarized (Fig. 1). Then FV were analyzed by using analyze particles function. The number (FVn), total area, and average area (FVav) of FV were obtained and “results” was saved as an .xls file and the maximum area (FVmax) of the FV (the largest FV area) was determined by sorting the areas of FVs. The percentage nonperfused choriocapillaris area (PNPCA), defined as the percentage of pixels in the choriocapillaris below a nonperfusion global threshold, was calculated by using the following formula: PNPCA (%) = (total area of FV / artifact excluded analysis area) × 100.[18, 19] All of these steps can be performed automatically with MATLAB based application of our algorithm (Fig. 4).

All steps, except binarization of en-face structural OCT image of outer retina, were re-perfomed to obtain FV image after removal of artifacts caused only by the superficial plexus (Fig. 2).

Exclusion criteria

Patients whose spherical equivalent refractive error was ≥ 4.0 diopters were excluded from the study. Any OCTA images with a quality score < 8 were excluded from analysis. One of the important points for this image processing method is to know that the Henle fiber layer can appear hyperreflective in OCT images if the retina is scanned with a decentered pupil entry position of OCT beam.[20] Because of the hyperreflective Henle fiber layer, segmentation errors may occur and healthy tissue may appear more

hyperreflective in en-face structural OCT images of the outer retina. Small segmentation errors due to the Henle fiber layer were corrected manually. Images with large segmentation errors were excluded.

Statistical analysis

All statistical analyses were performed with SPSS (version 21, IBM corp., Armonk, New York, USA). The Wilcoxon signed ranks test was used to compare FV measurements obtained before and after using our algorithm. The intraclass correlation coefficient were also calculated. $P < 0.05$ was considered statistically significant.

Results

There were three eyes with autosomal dominant drusen and 12 eyes with drusen secondary to non-exudative AMD in the drusen group. SRF group included 15 eyes with active CSC. The patients with SRF had a mean age of 47.3 ± 9.9 years old (min: 36, max: 65) and the patients with drusen had a mean age of 65.3 ± 15.1 years old (min: 37, max: 83). Five patients (33.3%) in SRF group and seven patients (46.7%) in drusen group were female.

PNPCA, FVav, FVmax, and FVn obtained using our algorithm were significantly lower than those obtained by removing only SCP in both groups (all $p < 0.05$) (Table).

Of 30 eyes participated in our study, 19 had vitreous opacities causing shadowing artifact. Our algorithm was able to remove artifacts due to vitreous opacities in 18 (94.7%) eyes. 12 eyes had serous PED and our algorithm removed all serous PEDs causing shadowing effect on choriocapillaris.

Discussion

With OCTA, it is possible to display SCP, deep capillary plexus, and choriocapillaris separately. Although OCTA provides cross-sectional images, visualization of deep layers, especially the choriocapillaris, is influenced by other tissues and alterations above them. These artifacts may cause overestimation of nonperfuison areas of choriocapillaris. [16, 21, 22] Commercial softwares of OCTA devices can remove artifacts secondary to SCP but they can not remove other artifacts. En-face OCT is very useful to show structural changes of retina. We used en-face structural OCT images of the outer retina to remove hyperreflective and hyporeflective artifacts because the fovea includes only the outer retinal layers while en-face OCT images of other layers have relatively higher hyporeflective foveal appearance, which makes these layers unsuitable for image binarization. Moreover, we observed that isoreflective lesions found in the en-face structural OCT images of outer retina do not lead to masking or unmasking artifacts. As expected, our study revealed that FVn obtained by removal of hyperreflective and hyporeflective artifacts on en-face structural OCT of the outer retina in addition to artifacts secondary to SCP is lower than FVn obtained by removing only SCP. We also detected a decrese of PNPCA, FVav, and FVmax after using our method in eyes with drusen and SRF.

In eyes with CSC, Aggarwal et al.[21] reported that the shadowing effect of overlying subretinal fluid, sub-RPE fluid and sub-RPE deposits hinders determination of real choriocapillaris FV. Yang et al.[22] found a positive correlation between central subfield thickness and choriocapillaris FV in CSC eyes with subretinal fluid due to its shadowing effect and vice versa in CSC eyes without subretinal fluid. Several studies have investigated choriocapillaris flow alterations in eyes with CSC but none of them has overcome OCTA visualization artifacts.[15, 21–26]

Some studies have been conducted in patients with AMD to obtain choriocapillaris images with drusen artifact removed.[13, 16, 18, 19] Borrelli et al.[18] used binarized RPE elevation images to exclude areas with drusen. However, using this method causes exclusion of all RPE lesions and some of these lesions do not lead to artifact. Nesper et al.[13] obtained drusen-artifact-removed choriocapillaris images with binarized en-face structural OCT images of the RPE layer. Only hyporeflective artifacts in en-face structural OCT can be removed by using their method, but most of the RPE lesions cause hyperreflective artifacts in en-face structural OCT of the RPE or outer retina. Using RPE elevation map, Zhang et al.[16] managed to compensate for signal reduction secondary to drusen without excluding any area. They reported decrease of FV after signal compensation. Artifacts due to very dense and shallow lesions can not be compensated as much as artifacts due to light and elevated lesions, because their method considered height but not density of RPE alterations. Their method can overcome artifacts due to sub-RPE fluid but can not overcome artifacts due to subretinal fluid and vitreous opacities. To the best of our knowledge, none of the previous automated methods can exclude or compensate for all artifacts due to subretinal fluid, PED, hyperreflective RPE lesions and vitreous opacities. We have overcome these artifacts by removing hyperreflective and hyporeflective artifacts on en-face structural OCT of the outer retina and keeping isoreflective lesion areas which do not lead artifact. We applied global thresholding to reveal nonperfusion areas of choriocapillaris (step 3). Other thresholding methods, such as Phansalkar thresholding, can also be used with our artifact removal process instead of step 3. In a very recent report, Burnasheva et al.[27] manually removed hyporeflective and hyporeflective artifacts using en-face structural OCT image of the whole retinal slab to evaluate FV in eyes with CSC. However, healthy areas and artifacts are separated more clearly using en-face structural OCT image of the outer retina than using en-face structural OCT image of the whole retinal slab. Moreover, using an automated method avoids user-dependent bias.

This study only focused on the effect of artifact removal on FV parameters in eyes with RPE abnormalities and SRF. Further studies are required for investigating FV alterations in specific retinal diseases.

In conclusion, nonperfusion areas of choriocapillaris may be overestimated in eyes with RPE abnormalities and SRF. These areas can be removed using thresholded images of the outer retina en-face OCT scans. Our new artifact-removal strategy is useful in assessment of choriocapillaris FV in eyes with SRF, drusen, drusen-like deposits and sub-RPE fluid. Morover, artifacts secondary to vitreous opacities can also be removed by our strategy.

Declarations

Funding

No funds, grants, or other support was received.

Conflicts of interest/Competing interests

The authors have no relevant financial or non-financial interests to disclose.

Availability of data and material (data transparency)

Available if required

Code availability (software application or custom code)

Available in https://github.com/erdosty/OCRA/releases/tag/1.46

Authors' contributions

All authors contributed to the study conception and design. Material preparation, data collection, and analyses were performed by M. Giray Ersoz. Software code was written by Erdost Yildiz. The first draft of the manuscript was written by M. Giray Ersoz, and all authors commented on previous versions of the manuscript. All authors read and approved the final manuscript.

Ethics approval

All procedures performed in this study were in accordance with the ethical standards of the institutional and/or national research committee and with the 1964 Helsinki declaration and its later amendments or comparable ethical standards. The study protocol was approved by the Institutional Review Board of Sisli Memorial Hospital, Istanbul

Consent to participate

Informed consent was obtained from all individual participants included in the study.

Consent to publish

Not applicable

References

1. Nickla DL, Wallman J (2010) The multifunctional choroid. Prog Retin Eye Res 29:144–168. 10.1016/j.preteyeres.2009.12.002() :. **doi**

2. Cheung CMG, Lee WK, Koizumi H, Dansingani K, Lai TYY, Freund KB (2019) Pachychoroid disease. Eye (Lond) 33:14–33. 10.1038/s41433-018-0158-4() :. doi
3. Chung SE, Kang SW, Lee JH, Kim YT (2011) Choroidal thickness in polypoidal choroidal vasculopathy and exudative age-related macular degeneration. Ophthalmology 118:840–845. 10.1016/j.ophtha.2010.09.012() :. doi
4. Ersoz MG, Arf S, Hocaoglu M, Sayman Muslubas I, Karacorlu M (2018) Indocyanine Green Angiography of Pachychoroid Pigment Epitheliopathy. Retina 38:1668–1674. 10.1097/IAE.0000000000001773() :. doi
5. Imamura Y, Fujiwara T, Margolis R, Spaide RF (2009) Enhanced depth imaging optical coherence tomography of the choroid in central serous chorioretinopathy. Retina 29:1469–1473. 10.1097/IAE.0b013e3181be0a83() :. doi
6. Matsumoto H, Mukai R, Morimoto M, Tokui S, Kishi S, Akiyama H (2019) Clinical characteristics of pachydrusen in central serous chorioretinopathy. Graefes Arch Clin Exp Ophthalmol 257:1127–1132. 10.1007/s00417-019-04284-4() :. doi
7. McLeod DS, Grebe R, Bhutto I, Merges C, Baba T, Lutty GA (2009) Relationship between RPE and choriocapillaris in age-related macular degeneration. Invest Ophthalmol Vis Sci 50:4982–4991. 10.1167/iovs.09-3639() :. doi
8. McLeod DS, Lutty GA (1994) High-resolution histologic analysis of the human choroidal vasculature. Invest Ophthalmol Vis Sci 35:3799–3811 ()
9. Prunte C, Flammer J (1996) Choroidal capillary and venous congestion in central serous chorioretinopathy. Am J Ophthalmol 121:26–34. 10.1016/s0002-9394(14)70531-8() :. doi
10. Ramrattan RS, van der Schaft TL, Mooy CM, de Bruijn WC, Mulder PG, de Jong PT (1994) Morphometric analysis of Bruch's membrane, the choriocapillaris, and the choroid in aging. Invest Ophthalmol Vis Sci 35:2857–2864
11. Sasahara M, Tsujikawa A, Musashi K, Gotoh N, Otani A, Mandai M, Yoshimura N (2006) Polypoidal choroidal vasculopathy with choroidal vascular hyperpermeability. Am J Ophthalmol 142:601–607. 10.1016/j.ajo.2006.05.051() :. doi
12. Warrow DJ, Hoang QV, Freund KB (2013) Pachychoroid pigment epitheliopathy. Retina 33:1659–1672. 10.1097/IAE.0b013e3182953df4() :. doi
13. Nesper PL, Soetikno BT, Fawzi AA (2017) Choriocapillaris Nonperfusion is Associated With Poor Visual Acuity in Eyes With Reticular Pseudodrusen. Am J Ophthalmol 174:42–55. 10.1016/j.ajo.2016.10.005() :. doi
14. Chen FK, Viljoen RD, Bukowska DM (2016) Classification of image artefacts in optical coherence tomography angiography of the choroid in macular diseases. Clin Exp Ophthalmol 44:388–399. 10.1111/ceo.12683() :. doi
15. Matet A, Daruich A, Hardy S, Behar-Cohen F (2019) PATTERNS OF CHORIOCAPILLARIS FLOW SIGNAL VOIDS IN CENTRAL SEROUS CHORIORETINOPATHY: An Optical Coherence Tomography Angiography Study. Retina 39:2178–2188. 10.1097/IAE.0000000000002271() :. doi

16. Zhang Q, Zheng F, Motulsky EH, Gregori G, Chu Z, Chen CL, Li C, **de** Sisternes L, Durbin M, Rosenfeld PJ, Wang RK **(**2018**)** A Novel Strategy for Quantifying Choriocapillaris Flow Voids Using Swept-Source OCT Angiography. Invest Ophthalmol Vis Sci 59:203–211. **doi**:10.1167/iovs.17-22953
17. Gargouri F **(**2020**) Thresholding the Maximum Entropy**. **MATLAB Central File Exchange**. https://www.mathworks.com/matlabcentral/fileexchange/35158-thresholding-the-maximum-entropy. **Accessed December 26, 2020**
18. Borrelli E, Souied EH, Freund KB, Querques G, Miere A, Gal-Or O, Sacconi R, Sadda SR, Sarraf D (2018) Reduced Choriocapillaris Flow in Eyes with Type 3 Neovascularization and Age-Related Macular Degeneration. Retina 38:1968–1976. 10.1097/IAE.0000000000002198() :. **doi**
19. Borrelli E, Uji A, Sarraf D, Sadda SR (2017) Alterations in the Choriocapillaris in Intermediate Age-Related Macular Degeneration. Invest Ophthalmol Vis Sci 58:4792–4798. 10.1167/iovs.17-22360() :. **doi**
20. Staurenghi G, Sadda S, Chakravarthy U, Spaide RF, **International Nomenclature for Optical Coherence Tomography P** (2014) Proposed lexicon for anatomic landmarks in normal posterior segment spectral-domain optical coherence tomography: the IN*OCT consensus. Ophthalmology 121:1572–1578. 10.1016/j.ophtha.2014.02.023() :. **doi**
21. Aggarwal K, Agarwal A, Deokar A, Mahajan S, Singh R, Bansal R, Sharma A, Dogra MR, Gupta V, Group OS (2017) Distinguishing features of acute Vogt-Koyanagi-Harada disease and acute central serous chorioretinopathy on optical coherence tomography angiography and en face optical coherence tomography imaging. J Ophthalmic Inflamm Infect 7:3. 10.1186/s12348-016-0122-z() :. **doi**
22. Yang HS, Kang TG, Park H, Heo JS, Park J, Lee KS, Choi S (2020) Quantitative evaluation of choriocapillaris using optical coherence tomography and optical coherence tomography angiography in patients with central serous chorioretinopathy after half-dose photodynamic therapy. PLoS One 15:e0227718. 10.1371/journal.pone.0227718() :. **doi**
23. Cakir B, Reich M, Lang S, Buhler A, Ehlken C, Grundel B, Stech M, Reichl S, Stahl A, Bohringer D, Agostini H, Lange C (2019) OCT Angiography of the Choriocapillaris in Central Serous Chorioretinopathy: A Quantitative Subgroup Analysis. Ophthalmol Ther 8:75–86. 10.1007/s40123-018-0159-1() :. **doi**
24. Gal-Or O, Dansingani KK, Sebrow D, Dolz-Marco R, Freund KB (2018) INNER CHOROIDAL FLOW SIGNAL ATTENUATION IN PACHYCHOROID DISEASE: Optical Coherence Tomography Angiography. Retina 38:1984–1992. 10.1097/IAE.0000000000002051() :. **doi**
25. Rochepeau C, Kodjikian L, Garcia MA, Coulon C, Burillon C, Denis P, Delaunay B, Mathis T (2018) Optical Coherence Tomography Angiography Quantitative Assessment of Choriocapillaris Blood Flow in Central Serous Chorioretinopathy. Am J Ophthalmol 194:26–34. 10.1016/j.ajo.2018.07.004() :. **doi**
26. Demirel S, Ozcan G, Yanik O, Batioglu F, Ozmert E (2019) Vascular and structural alterations of the choroid evaluated by optical coherence tomography angiography and optical coherence tomography

after half-fluence photodynamic therapy in chronic central serous chorioretinopathy. Graefes Arch Clin Exp Ophthalmol 257:905–912. 10.1007/s00417-018-04226-6() :. doi

27. Burnasheva MA, Kulikov AN, Maltsev DS (2020) Artifact-Free Evaluation of Choriocapillaris Perfusion in Central Serous Chorioretinopathy. Vision (Basel) 5. doi:10.3390/vision5010003

Figures

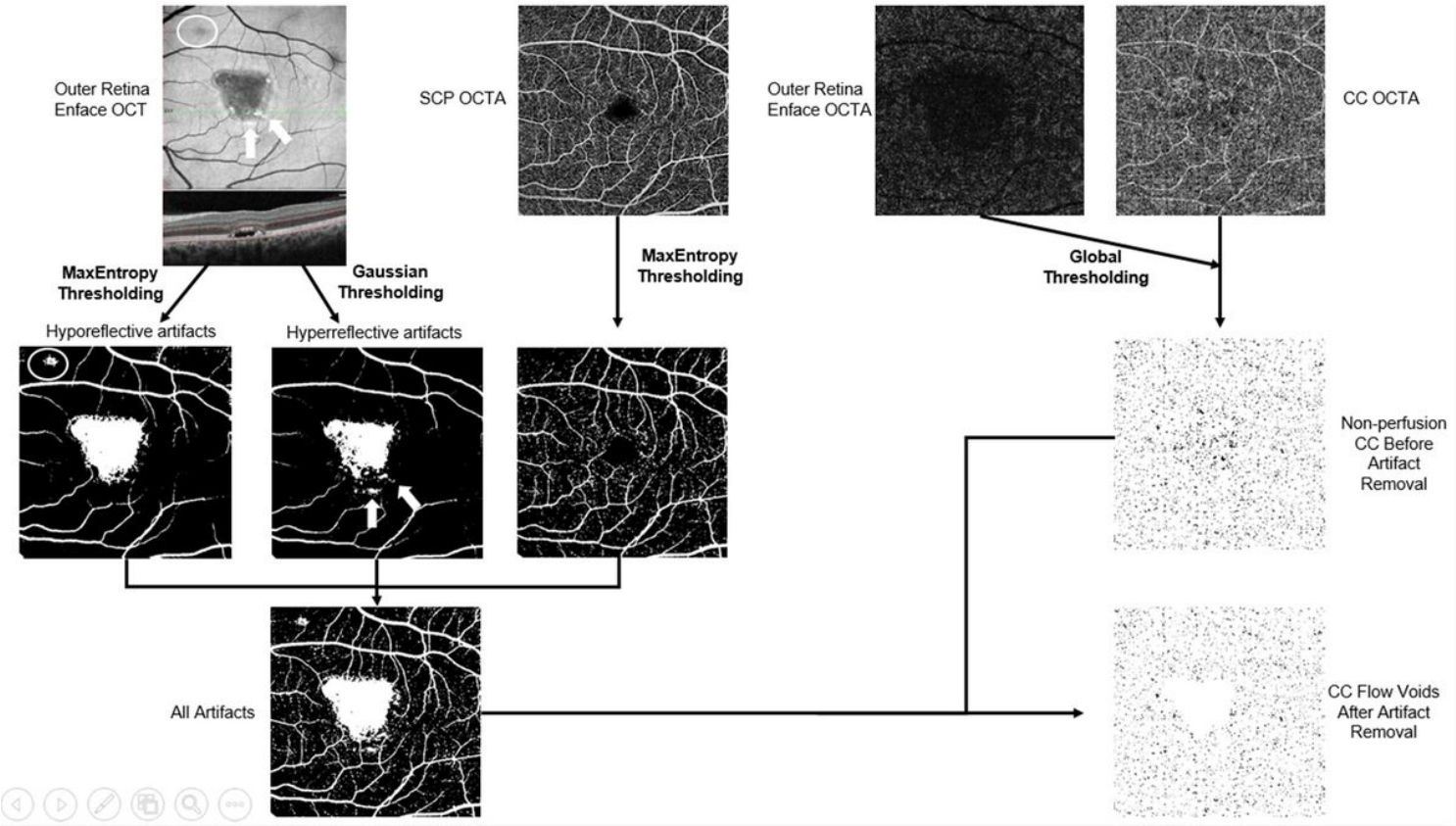

Figure 1

Representation of the algorithm used to obtain artifact removed choriocapillaris (CC) flow voids (FV) in an eye with active acute central serous chorioretinopathy. Before starting image processing, the edges of images were cut and 5 × 5 mm images centered on the fovea were imported into MATLAB. For image processing, we first applied two different thresholding to en-face optical coherence tomography (OCT) image of outer retina to determine the hyperreflective artifacts by gaussian distribution thresholding and the hyporeflective artifacts by maximum entropy thresholding. Hyporeflective areas due to retinal vessels, subretinal fluid, and vitreous opacities (white circles in the original and thresholded outer retina en-face OCT images) and hyperreflective areas (white arrows in the original and thresholded outer retina en-face OCT images) due to retinal pigment epithelium lesions and dense material accumulation appeared white in these thresholded images. Then we applied maximum entropy thresholding to OCT-angiography (OCTA) image of superficial capillary plexus (SCP). We merged these three thresholded images (hyporeflective artifacts + hyperreflective artifacts on outer retina en-face OCT + SCP). Then we binarized

this combined image and obtained an image in which all artifacts appeared white. To determine the global threshold of nonperfusion, the mean of the all pixel values in the outer retina en-face OCTA image was calculated and global thresholding was applied to CC image by using this value. Finally, threshold applied images of artifacts and the nonperfusion CC image were merged and binarized so we obtained the artifact removed CC FV image in which FVs appeared black. Note that the flow voids co-localized with the artifacts were removed.

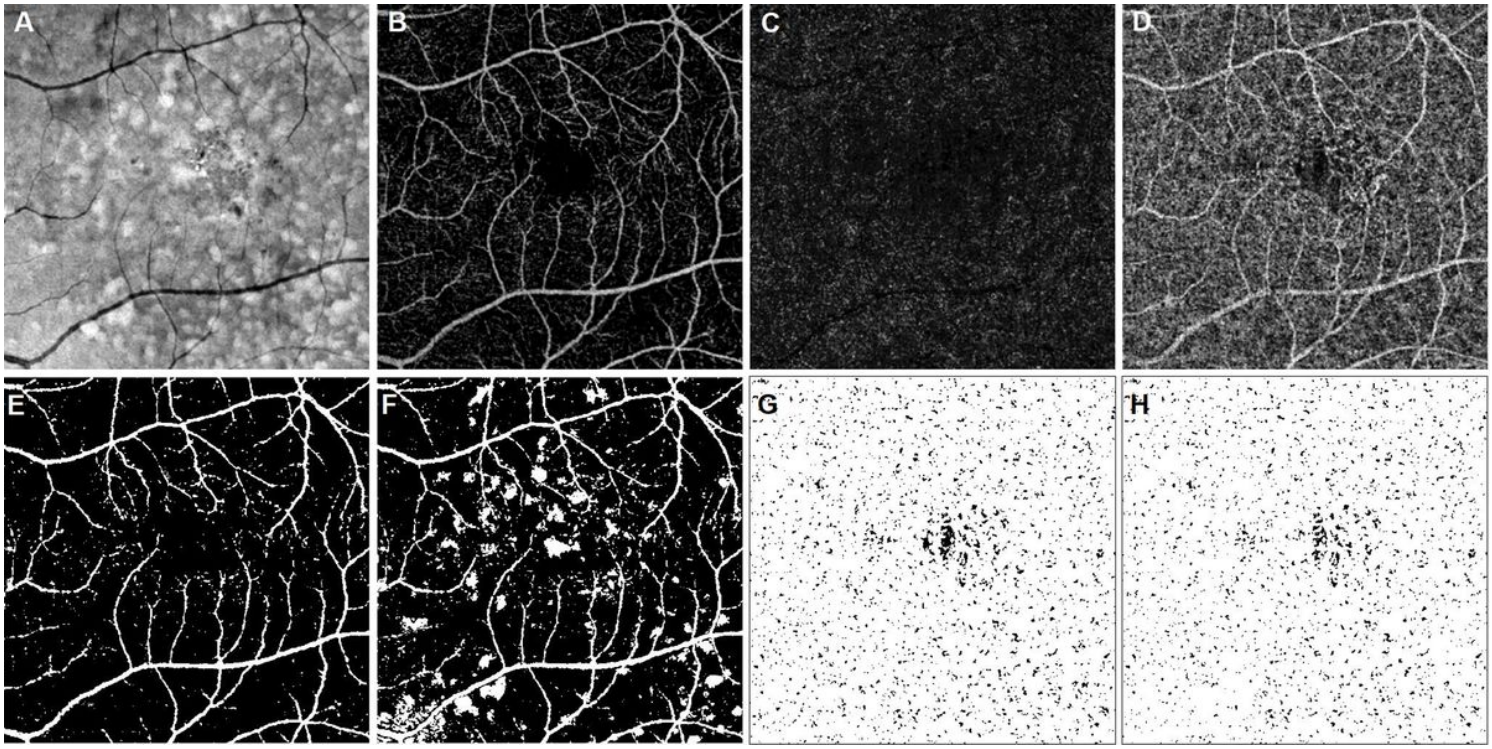

Figure 2

Image processing of choriocapillaris (CC) flow void analysis in an eye with drusen. A. En-face structural optical coherence tomography (OCT) image. B. En-face OCT angiography (OCTA) image of superficial plexus. C. En-face OCTA image of outer retina. D. En-face OCTA image of CC. E. Maximum entropy thresholded image of en-face OCTA image of superficial plexus. This image also represents the image that contains only the artifacts (white areas) secondary to the superficial plexus. F. The image that includes all artifacts (white areas). G. Flow voids (black areas) after removal of artifacts caused only by the superficial plexus (E). H. Flow voids (black areas) after removal of all artifacts (F).

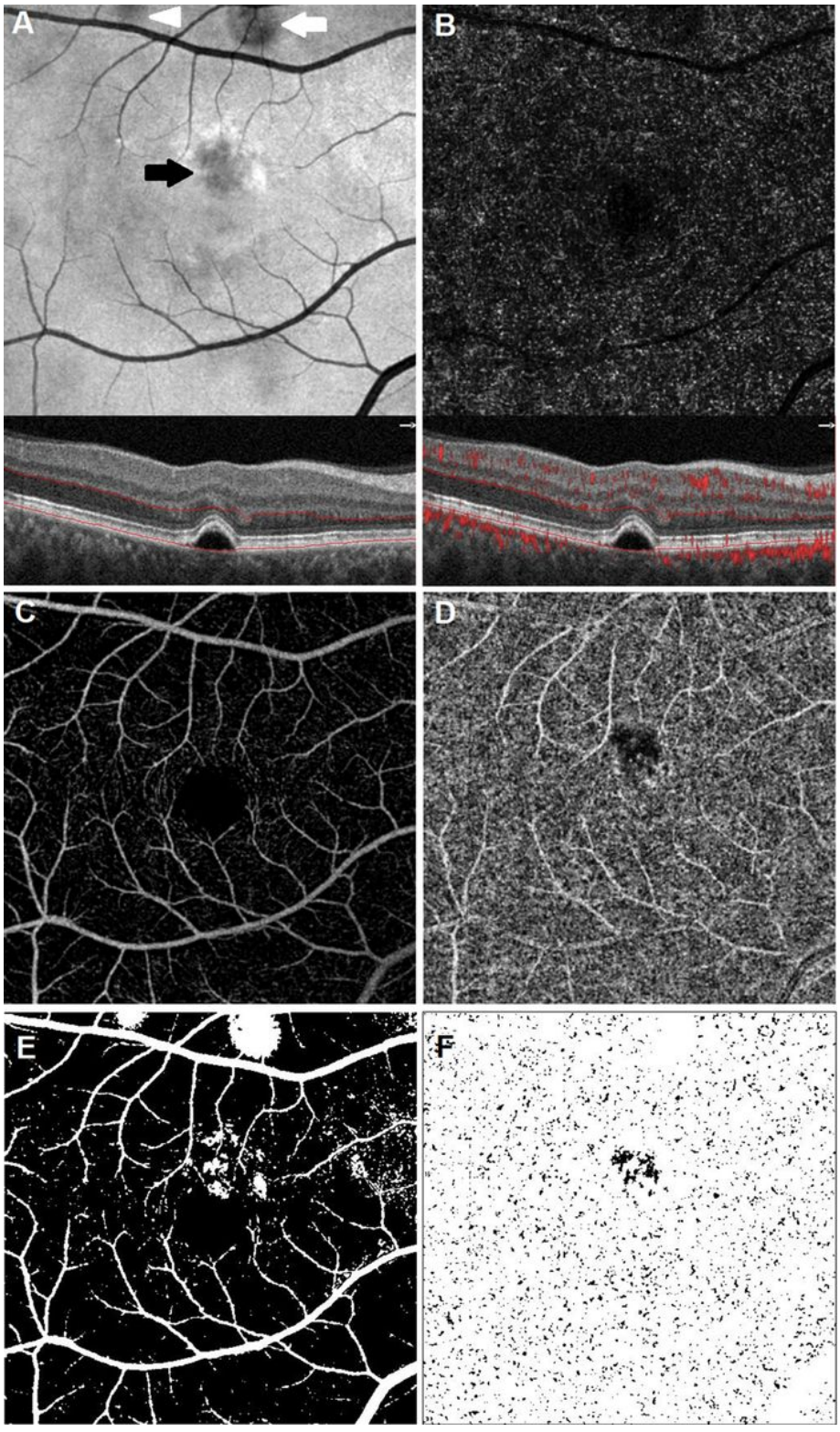

Figure 3

Image processing of choriocapillaris (CC) flow void analysis in an eye with subretinal fluid (white arrow), pigment epithelial detachment (black arrow), and vitreous opacity (white arrowhead). A. En-face structural optical coherence tomography (OCT) image and B-scan structural OCT images of outer retina. B. En-face OCT angiography (OCTA) image and B-scan structural OCT images of outer retina. C. En-face OCTA image of superficial plexus. D. En-face OCTA image of CC. E. The image that includes all artifacts

(white areas). Note that the artifacts secondary to subretinal fluid, pigment epithelial detachment, and vitreous opacity appear white. F. Flow voids (black areas) after removal of all artifacts.

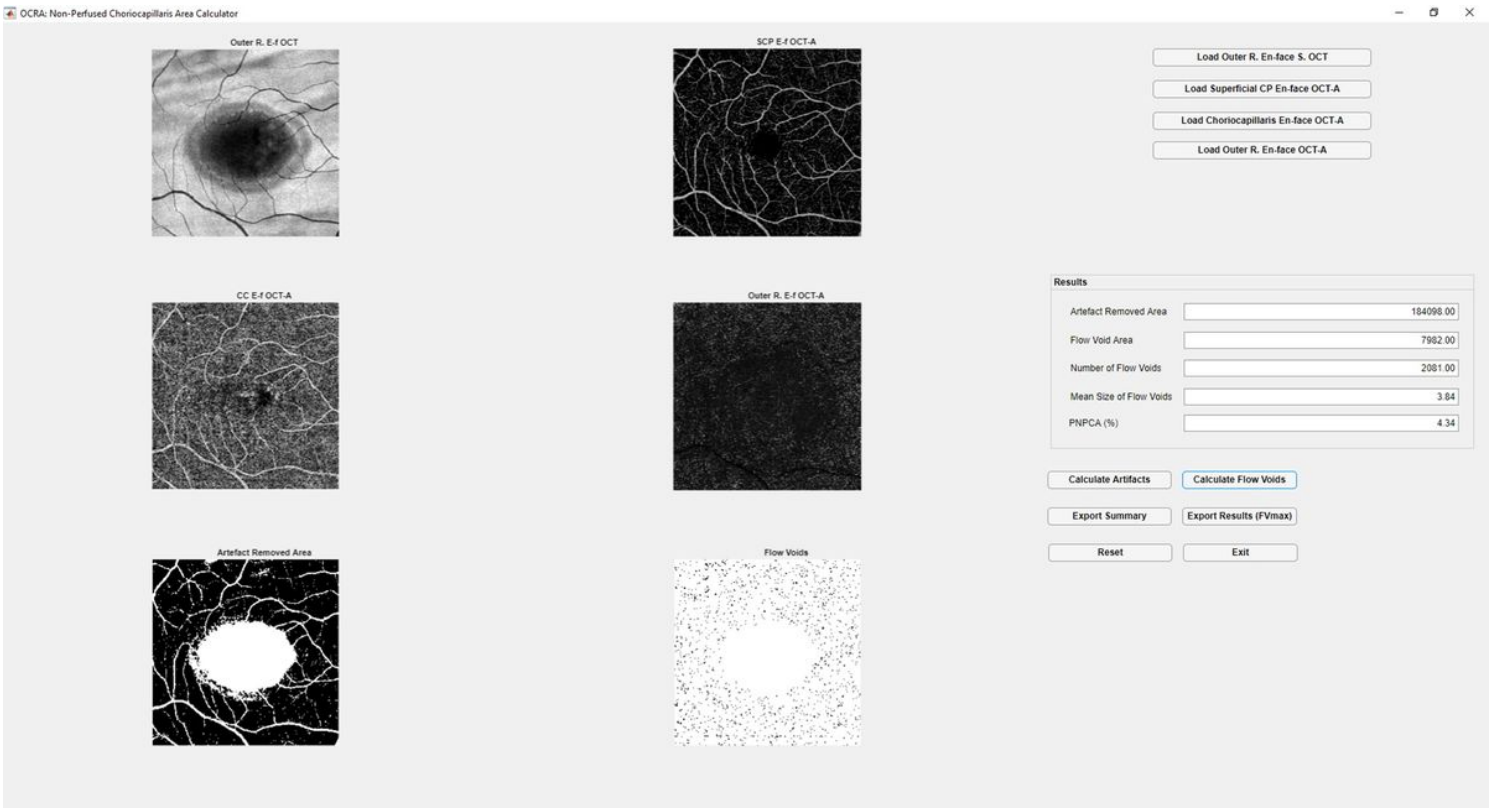

Figure 4

Automated image processing with our strategy using MATLAB based application in an eye with subretinal fluid. The user can load en-face structural optical coherence tomography (OCT) image of outer retina, superficial capillary plexus (SCP) OCT-angiography (OCTA) image, choriocapillaris OCTA image, and outer retina OCTA image. “Calculate artifacts” option generates “Artifact Removed Area” image in which artifacts appear white. It also calculates artifact removed area in pixel value (1 pixel = 10 µm, 1 pixel2 = 100 µm2). “Calculate Flow Voids” option generates “Flow Voids (artifact removed)” image and also calculates flow void area, number of flow voids, average (mean) size of flow voids and the percentage nonperfused choriocapillaris area (PNPCA). The maximum size of flow void areas can be obtained from “Export Results (FVmax)” option.